Ductile flow of methane hydrate

William B. Durham, Laura A. Stern, and Stephen H. Kirby

Abstract: Compressional creep tests (i.e., constant applied stress) conducted on pure, polycrystalline methane hydrate over the temperature range 260–287 K and confining pressures of 50–100 MPa show this material to be extraordinarily strong compared to other icy compounds. The contrast with hexagonal water ice, sometimes used as a proxy for gas hydrate properties, is impressive: over the thermal range where both are solid, methane hydrate is as much as 40 times stronger than ice at a given strain rate. The specific mechanical response of naturally occurring methane hydrate in sediments to environmental changes is expected to be dependent on the distribution of the hydrate phase within the formation — whether arranged structurally between and (or) cementing sediment grains versus passively in pore space within a sediment framework. If hydrate is in the former mode, the very high strength of methane hydrate implies a significantly greater strain-energy release upon decomposition and subsequent failure of hydrate-cemented formations than previously expected.

PACS No.: 62.20Fe

Résumé : Des essais de fluage sous compression (pression constante) conduits sur un hydrate polycristallin pur de méthane à des températures de 260 à 287 K et à des pressions de 50 à 100 Mpa, montrent que ce matériau est extraordinairement fort comparé à d'autres composés de glace. Le contraste avec de la glace d'eau hexagonale, parfois présentée comme ayant des propriétés similaires aux hydrates, est impressionnant : sur la gamme de température où les deux sont solides, l'hydrate de méthane est jusqu'à 40 fois plus fort que la glace à un taux donné de déformation. La réponse mécanique aux changements environnementaux de l'hydrate de méthane apparaissant naturellement dans les sédiments devrait dépendre de la distribution de la phase hydrate dans le formation – soit arrangée structurellement entre et/ou cimentant les grains de sédiments, vs passivement dans les espaces poreux dans le sédiment. Si l'hydrate est dans le premier état, la très grande force de l'hydrate de méthane suggère une libération significativement plus grande d'énergie de déformation lors de la décomposition et de la défaillance subséquente de la formation cimenté par l'hydrate que ce qu'on croyait précédemment.

[Traduit par la Rédaction]

Received 15 July 2002. Accepted 17 February 2003. Published on the NRC Research Press Web site at http://cjp.nrc.ca/ on ?? March 2003.

W.B. Durham.[1] University of California Lawrence Livermore National Laboratory, Livermore, CA 94550, U.S.A.
L.A. Stern and S.H. Kirby. U.S. Geological Survey, Menlo Park, CA 94025, U.S.A.

[1]Corresponding author (e-mail: durham1@llnl.gov).

 Proof/Épreuve

1. Introduction

Clathrate hydrates of natural gas are intermolecular compounds that occur naturally within both submarine continental margins and regions of Arctic permafrost. These materials occur in quantities sufficient to influence Earth's fossil fuel resource potential and to impact sea-floor stability and perhaps global climate issues [1–4]. Gas hydrate occurrences are also predicted in extraterrestrial settings as diverse as the polar caps of Mars [5], or within medium-to-large sized icy moons of the outer Solar System [6]. For example, methane hydrate was recently predicted to occur within the subsurface of Titan, Saturn's largest moon [7]. In the terrestrial environment, hydrocarbon hydrates are stable only under cold or subsurface conditions, usually mixed with marine sediments or Arctic permafrost. Successful sampling and property testing of pristine and unaltered gas-hydrate-bearing material from remote in situ settings continues to pose technological challenges, however, so direct, reliable characterization of gas hydrate physical properties and behavior remains poorly constrained. Accurate measurements of properties therefore presently require testing of well-characterized synthetic samples.

The response of natural gas hydrate formations to tectonic, gravitational, and (or) man-made forces is governed by a number of factors, including the mechanical strength of hydrate, the geometric distribution of the phases present (sediment, gas hydrate, water), fluid pressure, and the cohesion and frictional resistance between grains. Concentrations of distributed gas hydrate in formations identified as hydrate-bearing are poorly known, however, due to the difficulties in making direct observations and (or) reliable interpretations of partially-preserved retrieved material. Recent estimates put the hydrate concentration as low as 1–2 vol% in marine sediments [8], or as high as several tens of percent in permafrost regions [9]. In deposits where hydrate is located structurally between sediment grains [10] or as cementation around contacting grains [11], grain-to-grain cohesion and frictional resistance, from which unconsolidated "soft" sediments derive their strength [12,13], can be affected. Even at low concentrations, intergranular hydrate may thus influence formation strength, depending on its articulation within the sediment host. At higher concentrations, we can expect a formation-strengthening effect from a solid phase in pores by analogy to strength enhancement in frozen soils [14] or from general theory and experience with rheologies of aggregate mixtures [15,16].

Until recently, evaluating the effects of hydrocarbon hydrates on sediment properties was difficult because many fundamental physical properties had not been directly measured on pure structure I (sI) methane hydrate, thought to be the principal hydrocarbon hydrate in nature [2,4]. We report here the results of exploratory measurements of the plastic yield strength and the laws governing ductile flow of pure methane hydrate at conditions relevant to natural hydrates. Details of the experimental techniques are reported elsewhere [17]; this report is primarily intended to highlight some key aspects and implications of the strength of methane hydrate, and to offer some possible physical chemistry explanations for its surprisingly different behavior than water ice.

2. Experimental methods

Compressional deformation experiments in the apparent steady-state flow regime [18] were conducted on laboratory-synthesized samples of nonporous, polycrystalline, methane hydrate in the structure I form. Cylindrical test specimens were initially synthesized from granular H_2O "seed" ice held under $P_{CH_4} > 27$ MPa and heated through the ice melting point to $T \sim 290$ K [19,20]. Our method produces >99% pure sI methane hydrate as-synthesized, with measured composition of $CH_4 \cdot mH_2O$ where $m = 5.89 \pm 0.01$ [20]. The resulting samples have porosity of $29 \pm 1\%$ prior to testing, but are sufficiently cohesive to allow cleaving, grinding, and handling during the subsequent jacketing process.

Compaction of samples to full density was then performed in a cryogenic triaxial gas apparatus using the cold-compaction methods at 170–180 K described previously by our group [19,20] (Figs. 1 and 2). One notable improvement in the compaction procedure over early experiments involved subsequent

Fig. 1. Jacketed samples of methane hydrate. (*a*) Before hydrostatic compaction; (*b*) after hydrostatic compaction at 100 MPa and 280 K; (*c*) after shortening by a factor of 0.119 under axial load; and (*d*) after shortening by 0.190. Uniform shortening and broadening of deformed samples in (*c*) and (*d*) confirms that P–T conditions were adequate to suppress macroscopic fracture. All samples had approximately the same starting length. Visible in each photograph is the indium encapsulation around the bottom steel end cap, the methane hydrate sample (between broken lines), and the top steel end cap. The images are all aligned at the top of the hydrate portion and are at the same scale. Scale bar is 20 mm. The narrowed column above the top end cap is part of the internal force gauge.

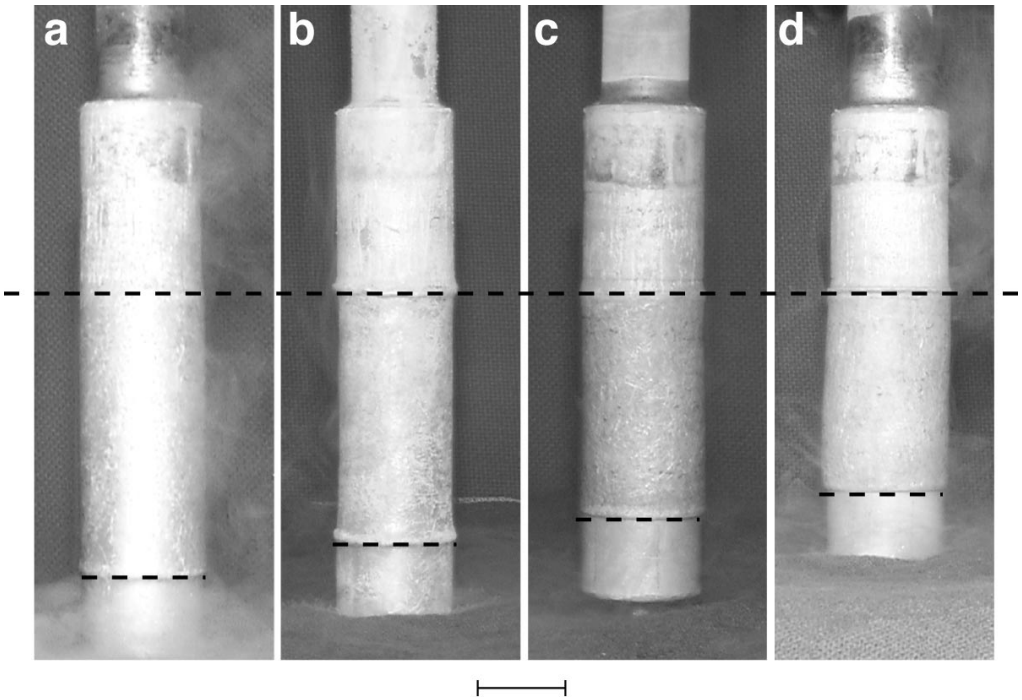

Fig. 2. A typical compaction curve for an initially 29% -porous methane hydrate sample, showing shortening (length change normalized by starting length) as a function of pressure at 175 K. Vertical arrow at right shows additional shortening achieved at 280 K under $P = 100$ MPa and $P_{CH_4} = 10$ MPa. Isotropic compaction of 29% -porous material corresponds to a shortening of 0.11 (horizontal broken line).

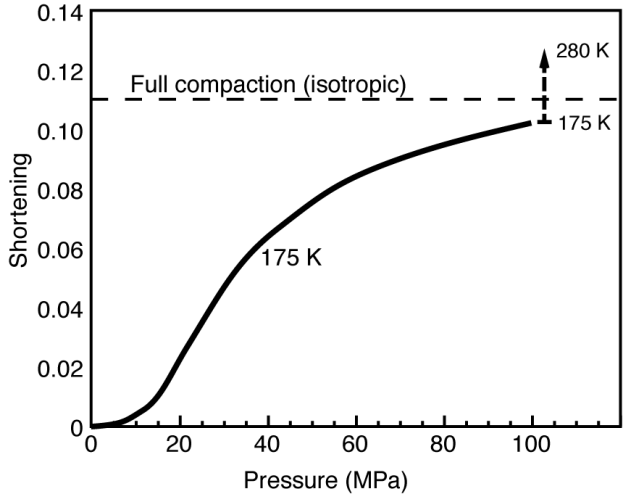

Fig. 3. Ductile flow behavior of methane hydrate. (*a*) Results from constant σ (creep) experiments, plotted as $\log \dot{\varepsilon}$ versus $\log \sigma$ at fixed pressure and shown here for several representative temperatures. P_{CH_4} is typically 10 MPa, raised to 15 MPa at 287 K. Continuous lines are a best fit at the labeled temperatures. (*b*) Comparison with water ice [21], with flow laws for each plotted as $\log \sigma$ versus $1/T$ at a fixed pressure of 50 MPa and fixed $\dot{\varepsilon} = 3.5 \times 10^{-7}$ s^{-1}. A change in flow mechanism for methane hydrate, i.e., a change in the slope of the flow law above $\sigma = 30$ MPa, is suggested by two preliminary measurements at very high stress [17]. There is great uncertainty in the upper part of this part of this curve.

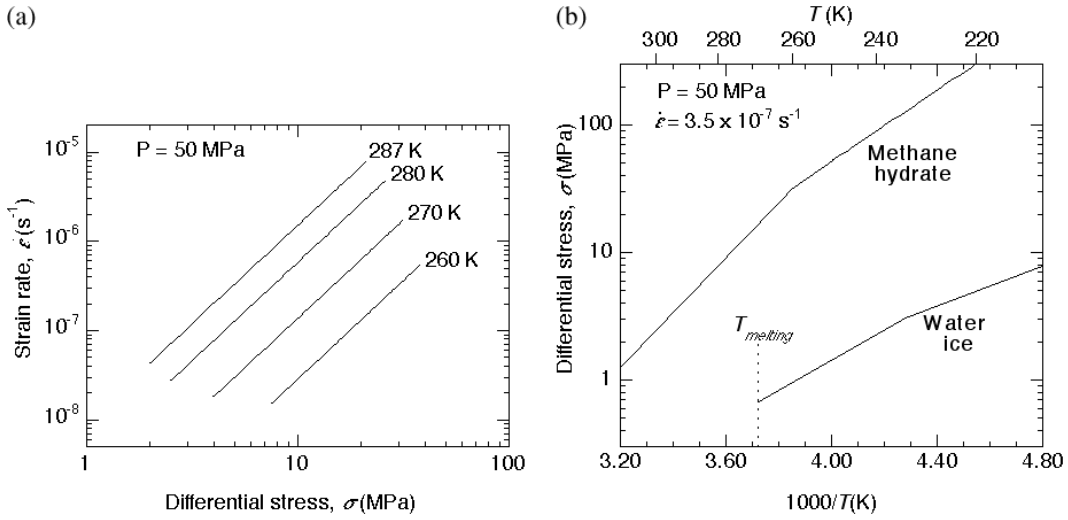

heating and continued pressurization to 280 K and 100 MPa to expel any free water in the samples (Fig. 2; see also ref. 17). We added this step because our previous findings showed significant water-ice development within methane hydrate samples during cold compaction and deformation procedures, even at conditions of pressure and temperature well within the nominal methane hydrate stability field [19,20]. The new procedure and apparatus configuration ensured sample maintenance within the methane hydrate stability field throughout all compaction and subsequent deformation procedures, while allowing expulsion of any free gas or liquid water that developed within samples during the experiments.

Samples were then tested in the triaxial apparatus by measuring strain rate ($\dot{\varepsilon}$) under creep conditions (constant differential stress) at confining pressures (P) of 50 and 100 MPa, methane pore pressures (P_{CH_4}) of 10 and 15 MPa, temperatures $260 \leq T \leq 287$ K, and differential stresses $5.7 \leq \sigma \leq 51.7$ MPa. We applied standard rock mechanics methods for all experiments, including sealing samples by jacketing with a soft metal and applying a gas-confining pressure to suppress macroscopic fracture [20,23].

3. Results and analysis

Curve fits for 20 creep measurements on five methane hydrate samples are shown in Fig. 3*a*. The steady-state rheology of most crystalline materials can be described by a mechanical equation of state or constitutive relationship [18] of the form

$$\dot{\varepsilon} = A\sigma^n \, \mathrm{e}^{-(E^* + PV^*)/RT} \tag{1}$$

where R is the gas constant and A, n, E^*, and V^* are flow parameters specific to the material in question. The best fit of the data to (1), represented in Fig. 3*a*, is $V^* = 19 \pm 10$ cm^3/mol; $E^* = 90\,000 \pm 6000$ J/mol; and $A = 10^{8.55}$ MPa^{-n} s^{-1}, $n = 2.2$, with a correlation coefficient of 0.80. More details of these

measurements and data reduction methods can be found elsewhere [17]. This fit is compared graphically to that for ice in Fig. 3*b*. Preliminary experiments at very high stresses [17] suggest a possible change in flow parameters at $\sigma > 30$ MPa, giving rise to the knee in the methane creep law in Fig. 3*b*. Chou et al. [25] recently discovered that a sI–sII phase transformation in methane hydrate occurs near $P = 100$ MPa, but we observe that the rheologies at $P = 50$ and 100 MPa show the same dependence on T and σ (within the scatter of the data), suggesting that this transformation did not occur in our samples or has no significant affect on rheology.

Despite some data scatter [17], the overall result is unambiguous: methane hydrate is extraordinarily strong compared to ordinary water ice [21] as well as to other icy compounds [22–24]. The contrast with ice Ih is dramatic (Fig. 3*b*). At the range of experimental temperature overlap, 260 K to the ice melting point, methane hydrate is more than 20 times stronger than ice at the same steady-state strain rate. Put differently, under the same applied stress, ice will deform approximate 10^6 times faster than pure methane hydrate. Extrapolated to $T < 260$ K, the strength difference widens rapidly.

Previous yield strength measurements of methane hydrate [19] and of gas-hydrate-bearing sediment [26,27] have been interpreted as showing that the strength of hydrate is roughly comparable to that of ice. The response of test specimens in those studies may have been strongly influenced by impurities of residual liquid or solid H_2O in the sample starting material, by the development of a secondary H_2O ice phase during compaction and deformation procedures [19,20], or by a lack of sufficient confining pressure to suppress fracture. More recently, Winters et al. [28] showed that during the initial transient stage of deformation, Ottawa sand with pore-filling methane hydrate is significantly stronger than the same sand with pore-filling ice. The marked strength difference between methane hydrate and ice is also supported by other indirect observations in our laboratory

(1) pressures exceeding 10 MPa are required to initially compact as-synthesized, 29%-porous cylinders of methane hydrate (reflected in the low slope near the origin of the compaction curve in Fig. 2),

(2) full uniaxial compaction of granular methane hydrate at 253 K requires more than ten times the axial stress than that required to compact granulated ice [10], and

(3) in creep tests, layered ice + methane hydrate samples display far higher strain rates and total strains in ice-rich sections than in hydrate-rich sections (Fig. 4).

4. Discussion

The dramatic contrast in high-temperature ductile strength between ice and methane hydrate is at first glance surprising: ice itself is a relatively strong material at very high homologous temperature $T_h = T/T_{melting}$ [29], and has nearly the same density, oxygen–hydrogen bond angles, and bond lengths as methane hydrate [4]. Two key differences between these compounds, however, may offer insight into their different mechanical behavior. First, most crystalline metals and oxides (including ice) deform at $T_h > 0.5$ by the coordinated motion of crystalline defects (point defects, dislocations, and grain boundaries), typically rate-limited by diffusion [18]. Evidence suggests that the rate of molecular water diffusion may be as much as two orders of magnitude slower in sI methane hydrate than in ice [4], hence this compound should be more creep resistant than ice. Second, the large hydrate sI unit cell (cubic, cell parameter 1.20 nm, 46 water molecules per unit cell) has about twice the linear dimension of ordinary ice Ih (hexagonal, cell parameters $a = 0.45$ and $c = 0.76$ nm, four water molecules per unit cell) [4]. This size difference may make the glide and climb motions of dislocations, as well as self-diffusion, more difficult, thus increasing the resistance of the material to intracrystalline plastic deformation.

The high strength of pure sI methane hydrate has significant implications for the mechanical behavior of hydrate-bearing formations in both terrestrial and planetological environments. Even in settings

Fig. 4. The post-test appearance of a composite sample of water ice (top) and methane hydrate (bottom), illustrating the dramatically weaker rheology of ice. Scale bar is 25 mm. This extreme heterogeneity in deformation occurred because the top end of the sample was inadvertently warmed during jacket welding, causing the upper portion to decompose to ice plus methane gas (vented through the pore-pressure tubing). The sample column was shortened by a factor of 0.196 at 260 K and $\sigma \approx 3.5$ MPa, resulting in an axially averaged $\dot{\varepsilon}$ of approximately 5×10^{-5} s^{-1}. Ice under these conditions deforms at a rate of 1×10^{-4} s^{-1}, methane hydrate at about 3×10^{-9} s^{-1} (Fig. 3*a*). Data from this test were not used in the flow-law quantification.

where hydrate concentration is low, at high effective normal stresses (normal stresses minus pore pressure) frictional resistance and cohesion between sediment grains may be high enough that time-dependent plastic deformation within the weakest grains of the aggregate governs macroscopic strength.

By analogy with frozen soils, the markedly higher plastic flow strength of methane hydrate compared with that of water ice implies a much higher flow strength for hydrate/sediment aggregates compared to frozen soils. On Earth, large mass movements of hydrate-bearing sediments perhaps triggered by pore-pressure effects of gas hydrate decomposition [30,31], may have been amplified by the loss of high intrinsic strength associated with the removal (by decomposition) of hydrate from the sediments. On Mars, carbon dioxide hydrate has been implicated in the development of observed land forms [32]. Loveday et al. [7] recently suggested that a 100 km thick layer of sI methane hydrate exists near the surface of Titan. If true, the thermal structure of that moon could be profoundly different from those of ice/rock moons without a hydrate layer. The combined effects of high resistance to convective flow and unusually low thermal conductivity of the hydrate layer [33] could imply reduced heat transport from interior to surface, and hence warmer internal temperatures for Titan.

Our investigation of time-dependent plastic deformation of pure methane hydrate represents a necessary first step toward understanding the inelastic response of hydrate-bearing formations in complex settings. Controlled experiments on hydrate-sediment aggregates with well-characterized phase articulation are next required to determine the specific roles that gas hydrate rheology may play in governing the inelastic behavior of natural hydrate-sediment aggregates.

Acknowledgments

We are grateful to John Pinkston (U.S. Geological Survey) and Wu Zhang (currently at West Virginia University) for their advice and assistance during the course of these experiments. We also thank W. Waite and I.-M. Chou of the U.S. Geological Survey for reviewing an earlier version of the manuscript. This work was performed in part under the auspices of the U.S. Department of Energy by the Lawrence Livermore National Laboratory under contract W-7405-ENG-48, and by the Natural Gas Hydrate Program of the U.S. Department of Energy, National Energy and Technology Laboratory.

References

1. T.S. Collett. *In* Natural gas hydrate in oceanic and permafrost environments. *Edited by* M.D. Max. Kluwer, Dordrecht, The Netherlands. 2000. pp. 123–136.
2. K.A. Kvenvolden. Rev. Geophys. **31**, 173 (1993).
3. K.A. Kvenvolden. *In* Natural gas hydrate in oceanic and permafrost environments. *Edited by* M.D. Max. Kluwer, Dordrecht, The Netherlands. 2000. pp. 9–16.
4. E.D. Sloan. Clathrate hydrates of natural gases. 2nd ed. Marcel Dekker, New York. 1998.
5. S.L. Miller and W.D. Smythe. Science (Washington), **170**, 531 (1970).
6. J.I. Lunine and D.J. Stevenson. Astrophys. J. Suppl. **58**, 493 (1985).
7. J.S. Loveday, R.J. Nelmes, M. Guthrie, S.A. Belmonte, D.R. Allan, D.D. Klug, J.S. Tse, and Y.P. Handa. Nature (London), **410**, 661 (2001).
8. W.S. Holbrook, H. Hoskins, W.T. Wood, R.A. Stephen, and D. Lizarralde. Science (Washington), **273**, 1840 1996).
9. S.R. Dallimore and T.S. Collett. *In* Scientific results from JAPEX/JNOC/GSC Mallik 2L-38 gas hydrate research well, Mackenzie Delta, Northwest Territories, Canada. *Edited by* T.S. Collett. Geological Survey of Canada, Ont. 1999. pp. 31–43.
10. M.B. Helgerud. Ph.D. thesis, Stanford University, Palo Alto, Calif. 2001.
11. G. Guerin, D. Goldberg, and A. Meltse. J. Geophys. Res. **104**, 17781 (1999).
12. O. Martinson. *In* Geological deformation of sediments. *Edited by* A. Maltman. Chapman & Hall, London. 1994. pp. 127–165.
13. T. Mulder and J. Alexander. Sedimentology, **48**, 269 (2000).
14. O.B. Andersland and B. Ladanyi. Frozen ground engineering. Chapman & Hall, New York. (1994).
15. M.R. Handy. J. Struct. Geol. **16**, 287 (1994).
16. T.E. Tullis, F.G. Horowitz, and J. Tullis. J. Geophys. Res. **96**, 8081 (1991).
17. W.B. Durham, S.H. Kirby, L.A. Stern, and W. Zhang. J. Geophys. Res. Manuscription in preparation. **(Author: Any further information?)** (2003).

18. J.-P. Poirier. Creep of crystals. Cambridge University Press, New York. 1985.
19. L.A. Stern, S.H. Kirby, and W.B. Durham. Science (Washington), **273**, 1843 (1996).
20. L.A. Stern, S.H. Kirby, W.B. Durham, S. Circone, and W.F. Waite. *In* Natural gas hydrate in oceanic and permafrost environments. *Edited by* M.D. Max. Kluwer, Dordrecht. 2000. pp. 323–348.
21. W.B. Durham, S.H. Kirby, and L.A. Stern. J. Geophys. Res. (Planets), **102**, 16293 (1997).
22. W.B. Durham, S.H. Kirby, and L.A. Stern. *In* Solar system ices. *Edited by* M. Festou. Kluwer, Dordrecht. 1998. pp. 63–78.
23. W.B. Durham and L.A. Stern. Ann. Rev. Earth Planet. Sci. **29**, 295 (2001).
24. W.B. Durham, L.A. Stern, and S.H. Kirby. Geophys. Res. Lett. **26**, 3493 (1999).
25. I.-M. Chou, A. Sharma, R.C. Burruss, J. Shu, H.-K. Mao, R.J. Hemley, A.F. Goncharov, L.A. Stern, and S.H. Kirby. Proc. Nat. Acad. Sci. **97**, 13484 (2000).
26. I.Y. Cameron, Y.P. Handa, and T.H.W. Baker. Can. Geotech. J. **27**, 255 (1990).
27. V.R. Parameswaran, M. Pardis, and Y.P. Handa. Can. Geotech. J. **26**, 479 (1989).
28. W.J. Winters, W.F. Waite, W.P. Dillon, D.H. Mason, and I.A. Pecher. *In* 2nd Russian Conference on Geocryology, Russia. 2001.
29. D.J. Goodman, H.J. Frost, and M.F. Ashby. Philos. Mag. **43**, 665 (1981).
30. R.E. Kayen and H.J. Lee. Marine Geotech. **10**, 125 (1991).
31. C.K. Paull, W.J. Buelow, W. Ussler, III, and W.S. Boroski. Geology, **24**, 143 (1996).
32. J.S. Kargel, K.L. Tanaka, V.R. Baker, G. Komatsu, and D.R. MacAyeal. *In* Lunar and planetary science conference XXXI. Abstract # 1891. Lunar and Planetary Institute, Houston. 2000.
33. W.F. Waite, B.J. deMartin, S.H. Kirby, J.C. Pinkston, and C.D. Ruppel. Geophys. Res. Lett. **29**(24), 82-1 (2002).